

A mini-TOF photofragment translational spectrometer – photofragmentation of CF₃I at 281.73 nm

Zhixin Tian, Weibin Bi, Huadong Deng, Xu Wang, Zichao Tang, Qihe Zhu *

*State Key Laboratory of Molecular Reaction Dynamics, Center for Molecular Science, Institute of Chemistry,
Chinese Academy of Sciences, Beijing 100080, PR China*

Received 13 August 2004; in final form 13 August 2004
Available online 6 November 2004

Abstract

Using a very weak electric field to accelerate the photofragment ions, we have constructed a very simple photofragment translational spectrometer with only a 50 mm total flight path, but we can get photofragment translational spectra with high resolution. On this apparatus, we have performed the photodissociation of CF₃I at 281.73 nm, and the same laser will ionize I*(²P_{1/2}) via REMPI. Seven well-resolved vibrational peaks were obtained. Six of them are assigned to the umbrella vibrational mode $v_2 = 0-5$ states of photofragment CF₃. The average internal energy $\bar{E}_{\text{int}} = 1928 \text{ cm}^{-1}$ is about 21% of the available energy.

© 2004 Elsevier B.V. All rights reserved.

1. Introduction

For the study of the photodissociation dynamics of simple polyatomic molecules, the photofragment translational spectroscopy is an important method. From the measurements of the translational energy distribution and the angular distribution of the photofragments, one can get the internal state distribution of the photofragments, the properties of the transition state, the reaction channels, the reaction dynamics, etc. Wilson's group [1] developed the first photofragment translational spectrometer (PTS) with the molecular beam (MB), the laser beam, and the detector axis perpendicular to each other. Many research groups [2–5] developed similar PTS with rotatable molecular beam source for getting, in addition, the angular distribution of the photofragments. The rotatable apparatus can give high resolution TOF spectra [6], but it is quite complicated, in

need of a rotation mechanism for the molecular beam and the ultrahigh vacuum for the detector chamber. Chandler and Houston [7] developed the ion imaging technique for the photofragments, and they can get, not only the translational energy distribution, but also the angular distribution of the photofragments in a single run of experiment. Eppink and Parker [8] improved the ion imaging technique, and got the velocity map imaging with higher resolution. This improved velocity map imaging technique has been now widely used. We report here a mini-TOF PTS with a total flight path of only 50 mm, even much simpler than the velocity map imaging apparatus, but it can give high resolution results. In this Letter, we report the photofragmentation experiments of CF₃I on this mini-TOF PTS, giving vibrational state-resolved photofragment translational spectra.

2. Experimental

A schematic diagram of our experimental set-up is shown in Fig. 1. Its structure is similar to the

* Corresponding author. Fax: +86 10 62563167.
E-mail address: qhzhu@iccas.ac.cn (Q. Zhu).

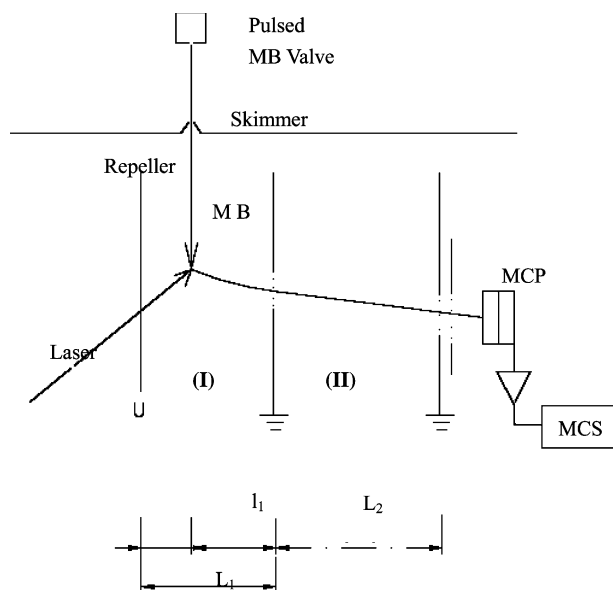
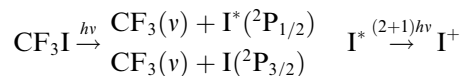


Fig. 1. Schematic diagram of our mini-photofragment translational spectrometer (MCP, micro channel plates; MCS, multi-channel scaler).

Doppler-selected time-of-flight technique of Liu's group [9], but with many differences (grounded extractor, no deflector, large cylindrical detection hole, extra detector grid plate, and shorter flight path). A sample of CF_3I (18% in mol) in the carrier gas Xe, with a stagnation pressure of 1 atm, is expanded through a 0.5 mm diameter nozzle of a pulsed valve (General Valve, 10 pps). We use the heavy carrier gas Xe to lower the velocity of the molecular beam V_{MB} (~ 355 m/s), so that the velocity spread and the angular spread of the molecular beam (MB) will give less effect to the resolution of our experiments. The gas after supersonic expansion is skimmed by a skimmer of 0.5 mm diameter, located 20 mm from the nozzle. The molecular beam flowing downward in the reaction chamber, is crossed perpendicularly by a focused laser beam with horizontal polarization (Fig. 1). The cross spot, i.e., the reaction zone, is 60 mm away from the hole of the skimmer. Both the source chamber and the reaction chamber are pumped with 500 l/s turbo molecular pumps. During experiments, the pressure is about 1×10^{-2} Pa in the source chamber and 5×10^{-5} Pa in the reaction chamber. The second harmonic (281.73 nm) of a dye laser, pumped by a YAG laser (Quanta-Ray), is used both for the photodissociation of CF_3I and for the ionization (REMPI) of the photofragment $\text{I}^*(^2\text{P}_{1/2})$



The photofragment ions I^+ are accelerated in region (I) by a weak electric field (< 5 V/2.55 cm) between the repeller plate and the grounded extractor plate. Then the ions, passing through the screen on the extractor

plate, fly freely in region (II) till reaching the detection plate, on which there is a detection hole with screen. We put an extra grid plate of low voltage (about 25 V) between the grounded detection plate and the high voltage micro channel plates (MCP), in order to diminish the electric field penetrating through the screen into the free flight region (II). The signal from the MCP is preamplified and recorded by a multi-channel scaler (SR430, Stanford Research System).

3. Results and discussion

Now, we discuss the flight of I^+ (Fig. 2). The motion of the fragment ion I^+ is composed of three parts $\vec{V} = \vec{V}_{\text{MB}} + \vec{V}_{\text{E}} + \vec{V}_{\text{CM}}$, (1) \vec{V}_{MB} , the constant downward motion with the molecular beam velocity V_{MB} , (2) \vec{V}_{E} , the horizontal motion accelerated by the electric field \vec{e} , and (3) \vec{V}_{CM} , the translational motion \vec{V}_{CM} in all directions from photofragmentation.

$$h\nu = D_0(C - I) + E_{\text{int}} + E_{\text{T}}, \quad E_{\text{T}} = \frac{1}{2}m_{\text{I}}V_{\text{CM}}^2 \times \left(\frac{m_{\text{CF}_3\text{I}}}{m_{\text{CF}_3}} \right).$$

(The Newton spheres in Fig. 2 correspond to the most probable internal state of the photofragments.) The center of the sphere (i.e., ions with $V_{\text{CM}} = 0$) moves along a parabola in region (I) and then moves along a straight line in region (II). We noticed that the spheres of the ions at different times in Fig. 2 are expanding spheres in the acceleration region (I), and in the free flight region (II), the spheres are not keeping spherical, but become gradually expanding into discus-like ellipsoid with the diameter in Z-axis unchanged. In order to get higher signal, we use a wide cylindrical detection hole with screen, tangential to the front surface of the discus-like ellipsoid.

The length of free flying region (II) ($L_2 = 35.0$ mm) is designed to be about twice of acceleration length ($l_1 = 15.0$ mm) in region (I). $L_2 = 2l_1$ is the space focus condition for the ions of $V_{\text{CM}} = 0$. For ions $V_{\text{CM}} \neq 0$, the space focus condition for the front ions is $L_2 = 2\left(l_1 + \frac{E_0}{\vec{e}}\right)$, where $E_0 = \frac{1}{2}m_{\text{I}}V_{\text{CM}}^2$ is the initial kinetic

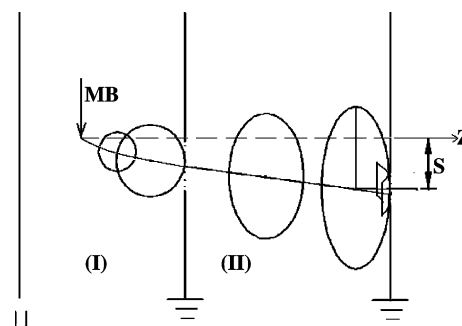


Fig. 2. Schematic diagram of the flight path of photofragment ions.

energy of the I^+ ions, and $\vec{e} = U/L_1$ is the electric field strength in region (I).

We take $S \cong 10$ mm (Fig. 2) and a cylindrical hole of 20×8 mm² with radius of curvature $R = 31$ mm. We tune the repelling voltage U around 4 V to get the TOF spectrum of I^+ ions with best resolution. At $U = 4.4$ V, the TOF spectrum of I^+ is given in Fig. 3. The fast high peak centered at 27 μ s corresponds to the front part of the discus-like ellipsoid. In this peak, the fine structures of several vibrational states are well-

resolved. The slow low peak centered at 38 μ s corresponds to the back part of the ellipsoid. Then we select $S \cong 12.5$ mm and a cylindrical hole of 22×10 mm² with radius of curvature $R = 37$ mm, and tune the repelling voltage U again for the highest resolution. At $U = 2.20$ V, the fine structure of the front peak of TOF spectrum of I^+ is shown in Fig. 4. Compared with the TOF spectrum at $U = 4.40$ V, the resolution is improved, but the signal noise ratio is lower. In this spectrum, there are seven well-resolved vibrational peaks, we assign six of

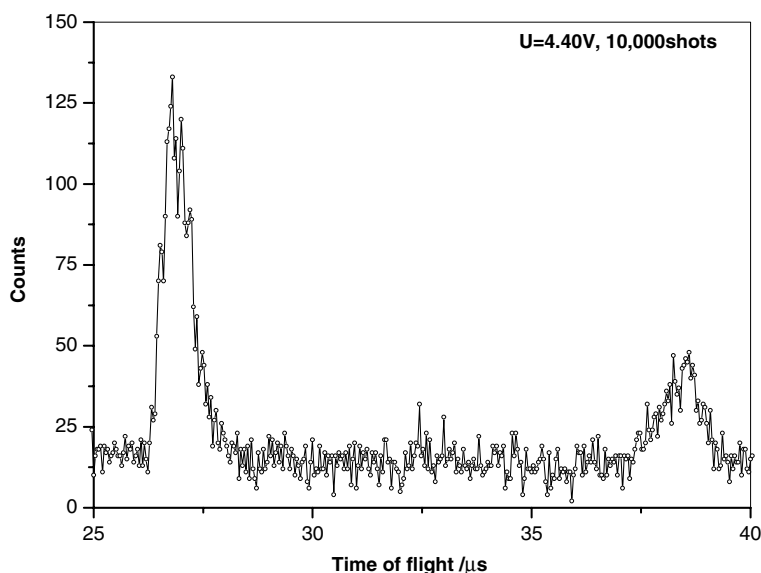


Fig. 3. Typical TOF spectrum of iodine from the photodissociation of CF_3I in I^* channel at 281.73 nm (repeller 4.40 V, channel width 40 ns, 10000 laser shots).

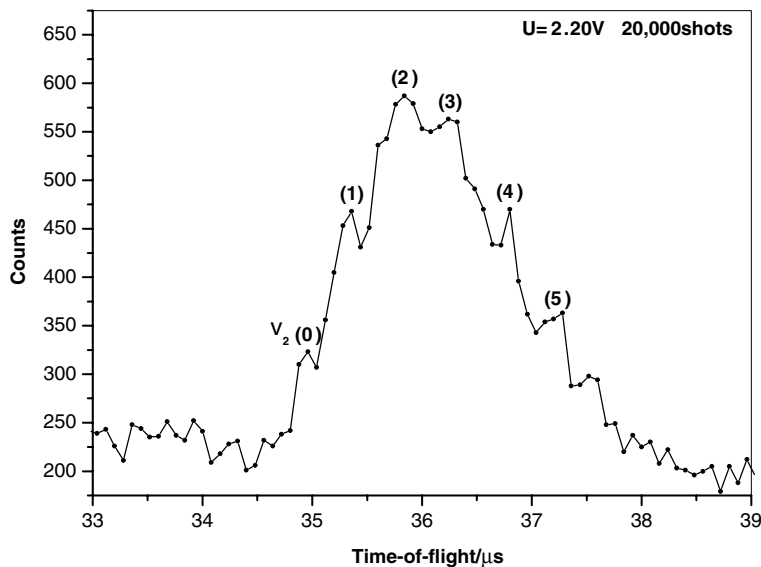


Fig. 4. Enlarged TOF spectrum of iodine from the photodissociation of CF_3I in I^* channel at 281.73 nm (repeller 2.20 V, channel width 80 ns, 20000 laser shots).

Table 1

The Vibrational energy and distribution of $\text{CF}_3(v_2)$ in the photofragmentation channel $\text{CF}_3\text{I} \xrightarrow{281.73 \text{ nm}} \text{CF}_3(v_2) + \text{I}^*(^2\text{P}_{1/2})$

| v_2 | Peak ^a (μs) | TOF corrected (μs) | ΔTOF (μs) | E_{T} (cm^{-1}) | E_{V} (cm^{-1}) | ΔE_{V} (cm^{-1}) | Fitted | | Population (%) |
|-------|-------------------------------------|---------------------------------|--------------------------------------|-------------------------------------|-------------------------------------|--|--|-------------------------------------|----------------|
| | | | | | | | ΔE_{V} (cm^{-1}) | E_{V} (cm^{-1}) | |
| 0 | 34.92 | 33.80 | | 9110 | 0 | | 701 | 0 | 5.5 |
| 1 | 35.32 | 34.20 | 0.40 | 8461 | 649 | 649 | 692 | 701 | 15 |
| 2 | 35.80 | 34.68 | 0.48 | 7725 | 1385 | 736 | 683 | 1393 | 24 |
| 3 | 36.28 | 35.16 | 0.48 | 7026 | 2084 | 699 | 674 | 2076 | 23.5 |
| 4 | 36.80 | 35.68 | 0.52 | 6313 | 2797 | 713 | 665 | 2750 | 17 |
| 5 | 37.28 | 36.16 | 0.48 | 5694 | 3416 | 619 | | 3415 | 10 |
| (1,4) | 37.56 | 36.44 | 0.28 | 5344 | 3766 | 350 | | (3836) | 5 |

^a Data from Fig. 4.

them to be the umbrella vibrational states $v_2 = 0-5$, (the fundamental $v_2 = 701 \text{ cm}^{-1}$). The seventh peak might be the ($v_1 = 1, v_2 = 4$) vibrational state.

From the population of the vibrational states (Table 1), we can get the average translational energy of photofragments $\bar{E}_{\text{T}} = 7182 \text{ cm}^{-1}$ and the average internal energy of CF_3 $\bar{E}_{\text{int}} = 1928 \text{ cm}^{-1}$. Our experimental value $\bar{E}_{\text{int}}/(\bar{E}_{\text{int}} + E_{\text{T}}) \cong 0.21$ at 281.73 nm is much higher than those of Aguirre and Pratt [10], ($E_{\text{int}}/(E_{\text{int}} + E_{\text{T}}) \cong 0.09$ at 280.99 nm and 0.08 at 286.71 nm), from their vibrational rings in the velocity map image, but it is comparable to that of Kim et.al. [11], ($E_{\text{int}}/(E_{\text{int}} + E_{\text{T}}) \cong 0.26$ at 277.38 nm). The large discrepancy in $E_{\text{int}}/(E_{\text{int}} + E_{\text{T}})$ between Pratt's group and ours might be due to the existence of the small $v_2 = 0$ vibrational peak in our photofragment translational spectra.

References

- [1] G.E. Busch, J.F. Cornelius, R.T. Mahoney, R.I. Morse, D.W. Schlosser, K.R. Wilson, Rev. Sci. Instrum. 41 (1970) 1066.
- [2] A.M. Wodtke, Y.T. Lee, J. Phys. Chem. 89 (1985) 4744.
- [3] M.D. Barry, P.A. Gorry, Mol. Phys. 52 (1984) 461.
- [4] Q. Zhu, S. Huang, et al., Acta Phys. Chim. Sinica 1 (1985) 211.
- [5] Q. Zhu, J. Cao, Y. Wen, J. Zhang, X. Zhong, Y. Huang, W. Fang, X. Wu, Chem. Phys. Lett. 144 (1988) 486.
- [6] X. Wang, Z. Tian, T. Shi, X. Shi, D. Yang, Q. Zhu, Chem. Phys. Lett. 380 (2003) 600.
- [7] D.W. Chandler, P.L. Houston, J. Chem. Phys. 87 (1987) 1445.
- [8] A.T.J.B. Eppink, D.H. Parker, Rev. Sci. Instrum. 68 (1997) 3477.
- [9] J.H. Wang, Y.T. Hsu, K. Liu, J. Phys. Chem. A 101 (1997) 6593.
- [10] F. Aguirre, S.T. Pratt, J. Chem. Phys. 118 (2003) 1175.
- [11] Y.S. Kim, W.K. Kang, K.H. Jung, J. Chem. Phys. 105 (1996) 551.